LETTER

doi:10.1038/nature10183

Transforming binding affinities from three dimensions to two with application to cadherin clustering

Yinghao Wu[1,2,3], Jeremie Vendome[1,2,3], Lawrence Shapiro[1,4], Avinoam Ben-Shaul[5] & Barry Honig[1,2,3]

Membrane-bound receptors often form large assemblies resulting from binding to soluble ligands, cell-surface molecules on other cells and extracellular matrix proteins[1]. For example, the association of membrane proteins with proteins on different cells (*trans*-interactions) can drive the oligomerization of proteins on the same cell[2] (*cis*-interactions). A central problem in understanding the molecular basis of such phenomena is that equilibrium constants are generally measured in three-dimensional solution and are thus difficult to relate to the two-dimensional environment of a membrane surface. Here we present a theoretical treatment that converts three-dimensional affinities to two dimensions, accounting directly for the structure and dynamics of the membrane-bound molecules. Using a multiscale simulation approach, we apply the theory to explain the formation of ordered, junction-like clusters by classical cadherin adhesion proteins. The approach features atomic-scale molecular dynamics simulations to determine interdomain flexibility, Monte Carlo simulations of multidomain motion and lattice simulations of junction formation[3]. A finding of general relevance is that changes in interdomain motion on *trans*-binding have a crucial role in driving the lateral, *cis*-, clustering of adhesion receptors.

It is commonplace to characterize binding between macromolecules quantitatively by measuring dissociation constants in solution, $K_d^{(3D)}$, which are typically defined in three-dimensional (3D) concentration units (for example moles per litre). However, phenomena that take place on membrane surfaces are dependent on two-dimensional (2D) densities and the relevant dissociation constants, $K_d^{(2D)}$, are defined in units such as molecules per square micrometre. Measurements of $K_d^{(2D)}$ are difficult to perform and have only been carried out in a small number of cases[4,5]. Thus, it would be extremely valuable to have a method that could transform measured values of $K_d^{(3D)}$ into corresponding values of $K_d^{(2D)}$. A reasonable simplifying assumption in such a method is that the binding interface formed by any two molecules is essentially identical in 3D and in 2D. The difference in the dissociation constants then results only from the change in dimensionality and from any other effects that arise from the constrained environment of a planar system.

It is possible to transform between two and three dimensions through the simple expression $K_d^{(2D)} = hK_d^{(3D)}$, where h is the 'confinement length'[6,7]. The basic idea is that if two interacting species are confined to a region of length h along an axis perpendicular to the plane of a membrane, then they are effectively confined to a volume Ah, where A is the area per molecule[6–8]. This simple procedure turns a 2D system into a 'quasi-3D system' because there is now a volume associated with each molecule even when it is constrained to a planar membrane. The extent of motion in the third dimension can arise from different factors such as molecular flexibility, rotations with respect to the membrane plane, membrane fluctuations and translational motion of the membranes themselves. A number of studies have used measured 3D and 2D affinities to determine h for individual systems. However, widely discrepant values have been obtained from the use of different methods to measure 2D affinities[5]; for example, fluorescence measurements typically yield values for h of the order of nanometres, whereas mechanical measurements have yielded values for h of the order of micrometres[5]. Here we focus on cases where two flat, parallel membranes are separated by a distance that allows proteins located on opposing surfaces to interact in *trans* and where proteins located on the same surface oligomerize in *cis*. The values of h that we find are of the order of nanometres, as is consistent with fluorescence measurements of 2D affinities[5].

Our specific focus is on the formation of ordered structures by the type I family of classical cadherins. Cadherins have five extracellular immunoglobulin-fold (EC) domains but the *trans*-binding interface is localized entirely on the membrane-distal EC1 domain[9]. We have recently shown that a molecular layer seen in crystal structures of classical cadherins corresponds to the extracellular structure of adherens junctions[10]. In addition to the *trans*-interface, a second, *cis*-, interface is formed between the EC1 domain of one cadherin and a region comprising parts of the EC2 and EC3 domains of another (Fig. 1). Cadherin *trans*-binding affinities have been measured in 3D solution[11]; binding affinities of *cis*-interactions are too weak to measure but have an upper limit of about 1 mM (ref. 10). We use this well-defined system as a basis for the development of general theoretical expressions that accomplish the transformation from 3D to 2D. These expressions, when used in conjunction with experimental data and our multiscale simulations, provide a detailed description of the structural and energetic basis of junction formation and elucidate new principles that are likely to be relevant to other systems.

Figure 2a describes the *trans*-dimerization reaction when cadherins are restricted to the membrane surface. As mentioned above, we assume that the binding interfaces are the same in solution and on a membrane surface, such that the energetic contributions to binding are identical: $\Delta E(3D) = \Delta E(2D)$. Hence, the difference in the binding affinities is entirely entropic. Because the *trans*-dimerization interface is located

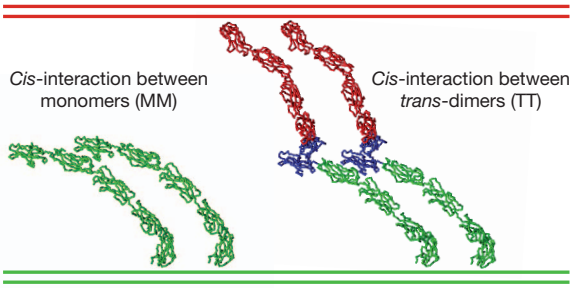

Figure 1 | Structures of *cis*-dimers formed from cadherin monomers and from *trans*-dimers. All coordinates are taken from the crystal structure of C-cadherin ectodomains[15]. *Trans*-dimers are formed by EC1 domains (blue) of cadherin monomers from lower (green) and upper (red) cell surfaces. Note that each *trans*-dimer structure has only a single *cis*-interface because the binding regions of the two monomers in a *trans*-dimer face in different directions. This property allows the formation of a 2D lattice in which each pair of *trans*-dimers makes only a single *cis*-interaction[3,10,15].

[1]Department of Biochemistry and Molecular Biophysics, Columbia University, New York, New York 10032, USA. [2]Howard Hughes Medical Institute, Columbia University, New York, New York 10032, USA. [3]Center for Computational Biology and Bioinformatics, Columbia University, New York, New York, 10032, USA. [4]Edward S. Harkness Eye Institute, Columbia University, New York, New York 10032, USA. [5]Institute of Chemistry and the Fritz Haber Research Center, The Hebrew University, Jerusalem 91904, Israel.

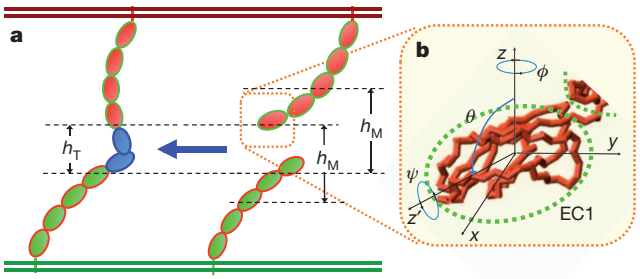

Figure 2 | Essential coordinates that characterize the dimerization processes of classical cadherins in a 2D membrane environment. **a**, The five domains of cadherin's extracellular regions are represented by ellipsoids. *Trans*-dimers (blue) can be formed from two cadherin monomers from two apposing cell surfaces. The molecules are free to diffuse in only two dimensions and rotational motion is constrained. A third dimension is introduced through variations in the perpendicular displacement from the membrane surface, defined by the variable h, which is different for the monomer and the *trans*-dimer. In general, h_M will be larger than h_T because *trans*-binding will limit molecular motion. **b**, The rotational degrees of freedom for EC1 domains are characterized by the three Euler angles, ϕ, θ and ψ.

on EC1, the difference between 3D and 2D affinities is related to the probability that two EC1 domains will encounter one another in an orientation that allows binding. This in turn depends on the local concentration of EC1 domains and on their freedom of rotational motion. As indicated in the figure, we use h_M and h_T to denote the ranges of EC1 motion normal to the membrane plane corresponding to monomeric and *trans*-dimeric cadherins, respectively. Thus, unlike in the expression $K_d^{(2D)} = hK_d^{(3D)}$ (refs 6, 7), we allow for different values of the monomer–dimer confinement length and, hence, their local concentrations, a factor that will prove crucial in the discussion below. To calculate h_M and h_T, we make the simplifying assumption that the two adhering membranes are flat and parallel to each other, as illustrated in Fig. 2. Assuming a cadherin density of 80 molecules per square micrometre[11], the lateral intermolecular distance is about 100 nm (and becomes much smaller once clustering begins). Estimates based on bending rigidity suggest that, over this lateral distance range, spontaneous fluctuations in membrane height are typically only a fraction of a nanometre[12,13], which is significantly less than the variations in h due to molecular flexibility considered in this work. Cells *in vivo* can extend membranous protrusions such as filopodia, which on some scale are not flat. Consideration of such issues goes beyond the scope of the current work; however, the treatment given here should provide a good starting point for these more complex instances.

The factors that enter into our treatment of rotational motion are shown in Fig. 2b, where the orientation of the EC1 binding site is described in terms of the three Euler angles, ϕ, θ and ψ. In 3D, all three rotational angles are unrestricted. By contrast, there are restrictions on the rotational freedom of the membrane-bound molecules except for rotations in ϕ, which corresponds to motion around the z axis. The rotational entropy is related to the integral over the three Euler angles[14], which yields $8\pi^2$ in 3D and a smaller value, $\Omega < 8\pi^2$, for membrane-bound molecules (Supplementary Information). Here $\Omega = (\Delta\omega_M)^2/\Delta\omega_T$, where $\Delta\omega_M = 2\pi\Delta\psi_M[1-\cos(\Delta\theta_M)]$ and $\Delta\omega_T = 2\pi\Delta\psi_T[1-\cos(\Delta\theta_T)]$ are the rotational phase space volumes of the monomer and the *trans*-dimer, respectively (Supplementary Information). Along with the confinement lengths h_M and h_T, $\Delta\omega_M$ and $\Delta\omega_T$ describe the 'confinement' in rotational motion in the constrained environment of the membrane.

In Supplementary Information, we derive the expression

$$\frac{K_d^{(2D)}(trans)}{K_d^{(3D)}(trans)} = \frac{\Omega}{8\pi^2}\frac{h_M^2}{h_T} = \frac{1}{8\pi^2}\frac{(\Delta\omega_M h_M)^2}{\Delta\omega_T h_T} \quad (1)$$

Equation (1) is quite general, although, as presented here, the variables refer specifically to the EC1 domains of cadherins. We note that it is straightforward to transform from 3D to 2D if h_M, h_T, $\Delta\theta_M$, $\Delta\psi_M$, $\Delta\theta_T$ and $\Delta\psi_T$ are known. These geometric variables will depend on the structures and flexibility of the proteins involved and on the constraints imposed by the membrane environment.

It is instructive to consider the special, hypothetical, case where the reactive EC1 domains of monomers and dimers can freely diffuse within the same 'reaction' volume, such that $h_M = h_T = h$ and, in addition, monomer and dimer rotations in 2D are totally unrestricted, as in 3D ($\Omega/8\pi^2 = 1$). In this case, equation (1) reduces to the simple expression of refs 6, 7, which, however, does not account for real differences in binding free energies in 2D and 3D. Real differences are due to two effects. First, because $h_M > h_T$ and $\Delta\omega_M > \Delta\omega_T$, the volume available to monomers in 2D is larger than that available to *trans*-dimers, implying that the binding affinity is smaller than in the 3D case. Second, the rotational entropy loss on binding in 2D is smaller than that in 3D, as quantitatively represented by $\Omega/8\pi^2 < 1$, resulting in enhancement of the binding affinity in 2D relative to 3D. These two effects will thus partly compensate each other, as demonstrated below in quantitative terms based on molecular-level simulations.

As mentioned above, many membrane receptors form lateral clusters on the cell surface driven by the formation of a distinct interprotein *cis*-interface[2], which for the specific case of cadherins has been characterized crystallographically[10,15]. Asymmetric *cis*-interfaces can form between two monomers, as well as between two *trans*-dimers, as shown in Fig. 1. In Supplementary Information, we derive equations for the 2D dissociation constants appropriate to the *cis*-dimerization of cadherin monomers, $K_d^{(2D)}{}_{MM}(cis)$, and *trans*-dimers, $K_d^{(2D)}{}_{TT}(cis)$. We show there that

$$\frac{K_d^{(2D)}{}_{MM}(cis)}{K_d^{(2D)}{}_{TT}(cis)} = \left(\frac{\Delta\omega_M h_M}{\Delta\omega_T h_T}\right)^2 \quad (2)$$

Equation (2), which accounts for differences in the strength of *cis*-interactions between monomers and *trans*-dimers, provides physical insights as to the coupling between *trans*- and *cis*-interactions. Even if *cis*-dimers formed from *trans*-dimers have an identical interface to that formed between monomers, the affinities will be different owing to differences in their respective rotational and vibrational flexibilities, as reflected by the factors $\Delta\omega_M/\Delta\omega_T$ and h_M/h_T, respectively. Qualitatively, because both factors are larger than one, it follows that the lateral attraction between *trans*-dimers is stronger than that between monomers.

In Methods, we describe a multiscale simulation approach that yields estimates of the six variables, h_M, h_T, $\Delta\theta_M$, $\Delta\psi_M$, $\Delta\theta_T$ and $\Delta\psi_T$, that define the transformation between 3D and 2D. It is evident from the simulations (Fig. 3) that *trans*- and/or *cis*-dimer formation places significant constraints on the molecular system. Values of h, $\Delta\theta$ and $\Delta\psi$ are reduced by a factor of approximately two to three in going from a monomer to a *trans*- or *cis*-dimer (that is, $h_T < h_M$, $\Delta\theta_T < \Delta\theta_M$ and $\Delta\psi_T < \Delta\psi_M$), an effect that will tend to weaken binding affinities (Supplementary Table 1). Supplementary Table 1 also shows 3D and 2D dissociation constants for the dimerization reactions occurring in solution and on the membrane. Notably, the values of $K_d^{(2D)}$ for *trans*-interactions reported in Supplementary Table 1 (ranging from 15 to 250 μm^{-2}) for N-cadherin are in the range obtained from measurements on molecules associated with the T-cell system[4,5,16], whereas those for E-cadherin are about an order of magnitude weaker owing largely to the greater values of $K_d^{(3D)}$.

The most drastic effect seen in the simulations is the difference in $K_d^{(2D)}$ of three to five orders of magnitude for lateral, *cis*-, dimerization affinities between monomers and *trans*-dimers. The increased binding affinity for *trans*-dimers has a clear physical explanation. The association of two cadherin monomers into a *cis*-dimer places severe constraints on the interdomain mobility of both ectodomains, such that

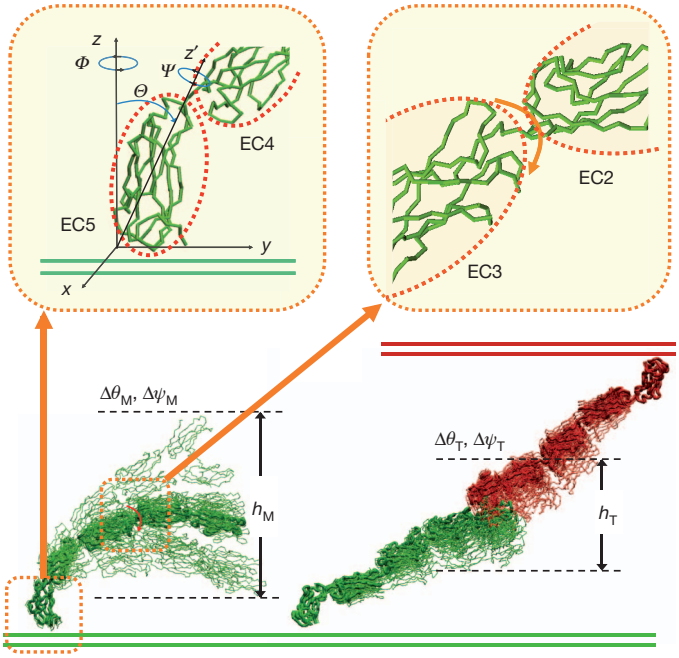

Figure 3 | Monte Carlo simulations of the flexibility of the cadherin ectodomain. The rotations of the EC5 domain with respect to the membrane plane depend on the three Euler angles, Φ, Θ and Ψ, of that domain, as shown in the upper left panel. The interdomain hinge motion, indicated by a red arrow, is shown in the upper right panel. The lower part of the figure shows the superposition of different monomer and *trans*-dimer conformations generated by the simulations. The range of values for h, $\Delta\psi$ and $\Delta\theta$ can be obtained from the statistical distribution of simulation results. The decreased flexibility of the *trans*-dimer with respect to the monomer is evident from the fact that h_T is less than h_M. Movies describing molecular motion of the monomers and dimers are included in Supplementary Information.

the range of allowable values of h, $\Delta\theta$ and $\Delta\psi$ is significantly reduced, thus resulting in a large entropic penalty for dimerization. By contrast, interdomain mobility is already reduced in *trans*-dimers, such that the additional entropic penalty associated with the *cis*-dimerization of two *trans*-dimers is small in comparison with that between monomers.

We have previously described the process of adherens junction formation as a phase transition between a dilute phase of monomers and *trans*-dimers that diffuse over the surface of a cell, and a condensed lattice composed of *trans*-dimers interacting laterally through a well-defined *cis*-interface[3]. Using lattice simulations, we showed that the formation of a condensed, ordered phase requires *trans*- and *cis*-interactions of sufficient magnitude. The results of such simulations, using the 2D binding affinities reported in Supplementary Table 1, illustrate the formation of well-defined lateral clusters (Fig. 4). Thus, converting the measured 3D cadherin binding affinities into 2D free energies yields interactions of sufficient strength to drive *trans*-dimer formation, and *cis*-interactions between *trans*-dimers of sufficient strength to drive the formation of ordered clusters of these dimers. That is, the values of $K_d^{(2D)}$ derived here from a combination of experiment, theory and simulation predict that cadherin ectodomains will form junctions, as is observed. By contrast, owing to the one-dimensional nature of *cis*-interactions between monomers (Fig. 1), and because of their small magnitude, monomer oligomerization is negligible[3].

It is important to note that the treatment we present is based entirely on forces localized to the extracellular region. This is justified for cadherins because junction-like structures form when cytoplasmic regions are deleted[10,17]. However, as has recently been demonstrated for T-cell receptor/major histocompatibility complex interactions, cytoskeletal forces can affect the kinetic and thermodynamic properties of extracellular domains[18]. Thus, although we expect cadherin junction formation *in vivo* to be affected significantly by cytoplasmic involvement, the process is almost certain to depend on the principles of ordered ectodomain assembly uncovered here.

Finally, the concepts and methods introduced in this work should facilitate the analysis of both *trans*- and *cis*-binding interactions between other flexible membrane-bound molecules. For example, chimaeras of CD48 with two or three additional immunoglobulin-like domains are ten times less efficient in adhesion than the wild-type protein, despite having the same binding interface as CD2 (ref. 19). The entropic penalty associated with restricting interdomain motion as a consequence of *trans*-binding provides a simple explanation of these observations and, more generally, offers a mechanism to control binding affinities of membrane-bound receptors that is not available to molecules that are free in solution.

METHODS SUMMARY

Monte Carlo simulations are carried out in which cadherins domains, each treated as a rigid body described at the level of Cα atoms, are allowed to move with respect to the membrane surface through random changes in the three Euler angles, Φ, Θ and Ψ, of the EC5 domain and through motions around the dihedral angles in the hinge regions as indicated in Fig. 3. The angle Φ ranges over 360°, whereas Θ and Ψ are restricted to a limited range (0° in one set of simulations and 30° in the

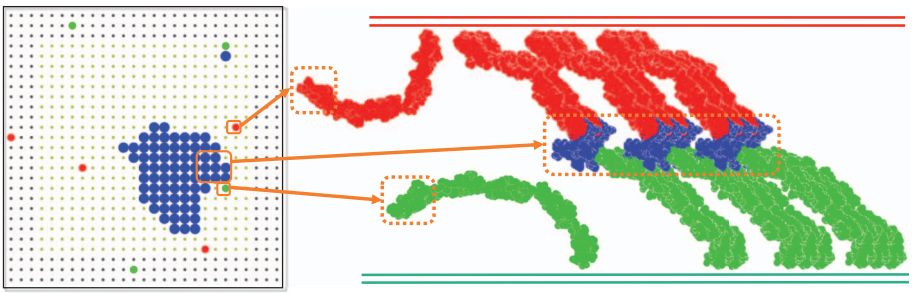

Figure 4 | Simulation of junction formation. The lattice in the left panel is a snapshot from a Monte Carlo simulation where cadherin monomers on apposing cells are coloured in red and green, respectively, and *trans*-dimers are coloured blue[3]. A diffusion trap mechanism[3] in which the trap region comprises 20 × 20 lattice sites (yellow/green), in the centre of a 2D lattice of 100 × 100 sites, with periodic boundary conditions, was used in the simulations. *Trans*-dimer formation can take place only in the trap region, as the distance between membranes in the surrounding region is too large to allow *trans*-dimer formation. The cadherins form ordered clusters in the trap region, as indicated. Details of the structure appear in ref. 10. A movie describing the formation of the ordered junction is included in Supplementary Information. The simulations are carried out using the value of $K_d^{(2D)}$(trans) for the *trans*-dimerization of E-cadherin (Supplementary Table 1) that is derived from experimental measurements. The total concentration of monomers in each of the two adhering surfaces (either free or *trans*-dimerized) is 1%, whereas the local concentration in the trap region is much higher (18.5%). The corresponding molecular structures of monomers on both cell surfaces, and part of the cluster formed by eight *trans*-dimers, are reconstructed in the right panel from the crystal structure of C-cadherin[15] using the same colour coding. The figure shows the Cα backbone with spheres placed on each carbon atom to improve clarity.

other). Motions around the flexible linker regions are described using the elastic network model[20,21], which defines normal modes along which interdomain motion is allowed. We applied the block normal mode approach[21,22] to partition the structure of the cadherin ectodomain into five rigid blocks, each corresponding to one extracellular domain. The six lowest-frequency modes, each of which describes a collective motion of the entire ectodomain, were used to generate alternative conformations. Fluctuations of the distances between the centres of mass were obtained from molecular dynamics simulations[23] and were used to calibrate the size of the Monte Carlo steps along the normal modes.

In each Monte Carlo step, the EC5 domain was allowed to rotate randomly and the conformation of the whole ectodomain was then changed along one of the normal modes starting with the C-cadherin monomer conformation. For *trans*- and *cis*-dimers, two ectodomains were first placed in conformations generated from the crystal structure of C-cadherin[15], after which Monte Carlo steps were taken. Two monomers were defined as forming a dimer if the root-mean-square distance obtained from a structural superposition was less than 6 Å, a value determined from molecular dynamics simulations[23] as preserving the dimer interface. Values of h_M, h_T, $\Delta\theta_M$, $\Delta\theta_T$, $\Delta\psi_M$ and $\Delta\psi_T$ were obtained directly from the conformations generated in the Monte Carlo simulations.

Full Methods and any associated references are available in the online version of the paper at www.nature.com/nature.

Received 28 December 2010; accepted 6 May 2011.

1. Aplin, A. E., Howe, A. K. & Juliano, R. L. Cell adhesion molecules, signal transduction and cell growth. *Curr. Opin. Cell Biol.* **11,** 737–744 (1999).
2. Aricescu, A. R. & Jones, E. Y. Immunoglobulin superfamily cell adhesion molecules: zippers and signals. *Curr. Opin. Cell Biol.* **19,** 543–550 (2007).
3. Wu, Y. *et al.* Cooperativity between trans and cis interactions in cadherin-mediated junction formation. *Proc. Natl Acad. Sci. USA* **107,** 17592–17597 (2010).
4. Dustin, M. L., Ferguson, L. M., Chan, P. Y., Springer, T. A. & Golan, D. E. Visualization of CD2 interaction with LFA-3 and determination of the two-dimensional dissociation constant for adhesion receptors in a contact area. *J. Cell Biol.* **132,** 465–474 (1996).
5. Dustin, M. L., Bromley, S. K., Davis, M. M. & Zhu, C. Identification of self through two-dimensional chemistry and synapses. *Annu. Rev. Cell Dev. Biol.* **17,** 133–157 (2001).
6. Bell, G. I. Models for the specific adhesion of cells to cells. *Science* **200,** 618–627 (1978).
7. Bell, G. I., Dembo, M. & Bongrand, P. Cell adhesion. Competition between nonspecific repulsion and specific bonding. *Biophys. J.* **45,** 1051–1064 (1984).
8. Chen, C. P., Posy, S., Ben-Shaul, A., Shapiro, L. & Honig, B. H. Specificity of cell-cell adhesion by classical cadherins: critical role for low-affinity dimerization through beta-strand swapping. *Proc. Natl Acad. Sci. USA* **102,** 8531–8536 (2005).
9. Patel, S. D. *et al.* Type II cadherin ectodomain structures: implications for classical cadherin specificity. *Cell* **124,** 1255–1268 (2006).
10. Harrison, O. J. *et al.* The extracellular architecture of adherens junctions revealed by crystal structures of type I cadherins. *Structure* **19,** 244–256 (2011).
11. Katsamba, P. *et al.* Linking molecular affinity and cellular specificity in cadherin-mediated adhesion. *Proc. Natl Acad. Sci. USA* **106,** 11594–11599 (2009).
12. Gov, N. S. & Safran, S. A. Red blood cell membrane fluctuations and shape controlled by ATP-induced cytoskeletal defects. *Biophys. J.* **88,** 1859–1874 (2005).
13. Zilker, A., Engelhardt, H. & Sackmann, E. Dynamic reflection interference contrast (RIC-) microscopy: a new method to study surface excitations of cells and to measure membrane bending elastic moduli. *J. Phys.* **48,** 2139–2151 (1987).
14. Hill, T. L. *An Introduction to Statistical Thermodynamics* 147–176 (Dover, 1987).
15. Boggon, T. J. *et al.* C-cadherin ectodomain structure and implications for cell adhesion mechanisms. *Science* **296,** 1308–1313 (2002).
16. Dustin, M. L. *et al.* Low affinity interaction of human or rat T cell adhesion molecule CD2 with its ligand aligns adhering membranes to achieve high physiological affinity. *J. Biol. Chem.* **272,** 30889–30898 (1997).
17. Hong, S., Troyanovsky, R. B. & Troyanovsky, S. M. Spontaneous assembly and active disassembly balance adherens junction homeostasis. *Proc. Natl Acad. Sci. USA* **107,** 3528–3533 (2010).
18. Huppa, J. B. *et al.* TCR-peptide-MHC interactions in situ show accelerated kinetics and increased affinity. *Nature* **463,** 963–967 (2010).
19. Milstein, O. *et al.* Nanoscale increases in CD2–CD48-mediated intermembrane spacing decrease adhesion and reorganize the immunological synapse. *J. Biol. Chem.* **283,** 34414–34422 (2008).
20. Atilgan, A. R. *et al.* Anisotropy of fluctuation dynamics of proteins with an elastic network model. *Biophys. J.* **80,** 505–515 (2001).
21. Li, G. H. & Cui, Q. A coarse-grained normal mode approach for macromolecules: an efficient implementation and application to $Ca2^+$-ATPase. *Biophys. J.* **83,** 2457–2474 (2002).
22. Tama, F., Gadea, F. X., Marques, O. & Sanejouand, Y. H. Building-block approach for determining low-frequency normal modes of macromolecules. *Proteins* **41,** 1–7 (2000).
23. Van Der Spoel, D. *et al.* GROMACS: fast, flexible, and free. *J. Comput. Chem.* **26,** 1701–1718 (2005).

Supplementary Information is linked to the online version of the paper at www.nature.com/nature.

Acknowledgements This work was supported by National Science Foundation grant MCB-0918535 (to B.H.) and National Institutes of Health grant R01 GM062270-07 (to L.S.). The financial support of the US-Israel Binational Science Foundation (grant no. 2006-401, to A.B.-S., B.H. and L.S.) and the Israel Science Foundation (ISF 1448/10 and 695/06) (to A.B.-S.) is acknowledged. We thank E. Sackmann for an email exchange concerning membrane fluctuations.

Author Contributions Y.W., J.V., L.S., B.H. and A.B.-S. designed the research; Y.W. performed the multiscale simulations; J.V. carried out the all-atom molecular dynamics simulations; Y.W., B.H. and A.B.-S. analysed the data; Y.W., A.B.-S. and B.H. contributed analytic tools; and Y.W., L.S., B.H. and A.B.-S. wrote the paper.

Author Information Reprints and permissions information is available at www.nature.com/reprints. The authors declare no competing financial interests. Readers are welcome to comment on the online version of this article at www.nature.com/nature. Correspondence and requests for materials should be addressed to A.B.-S. (abs@fh.huji.ac.il) or B.H. (bh6@columbia.edu).

METHODS

Modelling intramolecular conformational changes. We used the elastic network model[20] to define normal modes to be used in the Monte Carlo simulations. This model is based on the approximation that molecular vibrations near an equilibrium conformation can be determined by a coarse-grained harmonic potential

$$V = \frac{\gamma}{2}\sum_{ij}\sigma_{ij}\left(\left|\mathbf{r}_{ij}\right| - \left|\mathbf{r}_{ij}^{0}\right|\right)^{2}$$

$$\sigma_{ij} = \begin{cases} 1, & \left|\mathbf{r}_{ij}^{0}\right| \le r_{c} \\ 0, & \left|\mathbf{r}_{ij}^{0}\right| > r_{c} \end{cases}$$

where $\left|\mathbf{r}_{ij}\right|$ and $\left|\mathbf{r}_{ij}^{0}\right|$ are respectively the instantaneous and equilibrium values of the distance between Cα atoms i and j, γ is the uniform force constant and the cut-off value, r_c, is set as 13 Å. We applied the block normal mode approach[21,22] to partition the structure of each cadherin ectodomain into five blocks, each corresponding to one extracellular domain. A Cα representation of the native structure of C-cadherin[15] (Protein Data Bank ID, 1L3W) was used as an initial model. We chose the six lowest-frequency modes, all of which describe collective motions of the entire ectodomain. Amplitudes of motion along the direction defined by each normal mode were obtained from the following procedure.

Calibrating the amplitude of interdomain motions. A 40-ns all-atom molecular dynamics simulation of the EC1 and EC2 domains was carried out in explicit solvent using GROMACS[23]. For structures generated along the simulation trajectory, the coordinates of the EC2 domain were fixed and then the distance between the centre of mass of the EC1 domain in each simulation step and its centre of mass in the initial conformation was calculated. Supplementary Fig. 1a plots this distance versus simulation time. After transforming this fluctuation profile into a frequency-like histogram, a Gaussian-like distribution with a range of about ± 8 Å is obtained (Supplementary Fig. 1b).

To relate this distance fluctuation to corresponding motions along the six normal modes, we performed a series of Monte Carlo tests where we started with the crystal structure and generated a series of different conformations by taking a random step, smaller than some pre-chosen cut-off, along any one of the six eigenvectors. The centre of mass of EC5 was kept fixed, so that no 2D diffusion occurred in this stage. All conformations generated with a single Monte Carlo test have the same cut-off value. A total of 20 cut-offs were tried with the goal of finding a value (and a corresponding step size) that would reproduce, as closely as possible, the distribution of EC1–EC2 distances obtained from the molecular dynamics simulations. To this end, all normal-mode-generated structural models obtained using the same cut-off were aligned to one another by superimposing their EC2 domains, yielding an ensemble of EC1 domain positions. By calculating the distance between the EC1 domain centre of mass in each structural model and the EC1 domain centre of mass in the crystal structure, a histogram of this distance distribution was generated for each cut-off. The Monte Carlo step size along normal modes was defined so that the range of normal-mode-generated distance distributions was as close as possible to 8 Å (Supplementary Fig. 1c), the value generated by the all-atom simulations.

Estimating geometric variables of EC1 domain fluctuations. Different conformations of a cadherin monomer were generated with a Monte Carlo simulation using the normal modes and step sizes derived from the methods described above. In each step of the simulation, the EC5 domain is first allowed to randomly rotate within a small interval in Euclidean space Φ–Θ–Ψ, as shown in the upper left panel of Fig. 3. Then the conformation of the entire ectodomain is changed, in a positive or negative direction, along one of the six normal modes using a step size chosen randomly from the range of values that produce the distribution shown in Supplementary Fig. 1c. A large number of structures are generated in this way as shown in Fig. 3. The fluctuations of the centre of mass of the EC1 domains along the z axis, as well as fluctuations in the Euler angles, are obtained directly from a straightforward geometric analysis of these structures: h_M is defined as twice the standard deviation of the distribution of the centre of mass of the EC1 domain along the z axis, and the distributions of the Euler angles, defined by $\Delta\theta_M$ and $\Delta\psi_M$, are obtained in the same way. Results are shown in Supplementary Table 1 and Supplementary Fig. 2.

For a *trans*-dimer, two cadherin ectodomains are initially placed facing each other, as in the native structure of the *trans*-dimer of C-cadherin[15]. Then the conformation of each monomer is randomly modified using the algorithm described above for monomers. Intermolecular clashes are checked after each Monte Carlo step. If there is no severe intermolecular clash, and the distance between the centres of mass of the two EC1 domains is less than 50 Å, the root mean-square distance (r.m.s.d.) of the EC1 domain pair relative to the native strand-swapped-dimer is calculated. Two cadherin monomers are defined as forming a *trans*-dimer if the EC1 r.m.s.d. is less than 6 Å. This cut-off value was determined from all-atom molecular dynamics simulations of a *trans*-dimer formed by C-cadherin EC1–EC2 domains. During the molecular dynamics simulations, the dimer structure deviated from the initial conformation as, for example, can be seen in Supplementary Fig. 3, which shows a structural superposition of two conformations, one in the initial state (red) and one chosen from the middle of the simulation (green). The Cα r.m.s.d. between the two EC1 domains is about 4 Å. Supplementary Fig. 3b shows two independent trajectories of EC1 r.m.s.d. fluctuations obtained from the GROMACS[23] molecular dynamics simulations. As can be seen in the figure, the r.m.s.d. fluctuations from the native structure are within the range of 6 Å in both simulations.

The range of EC1 domain fluctuations along the z axis, h_T, and the rotational distribution, $\Delta\theta_T$ and $\Delta\psi_T$, were determined and are reported in Supplementary Table 1 and Supplementary Fig. 4. The procedure was the same as used for monomers except that the fluctuations of each EC1 domain in a *trans*-dimer were included separately in the distribution. The same procedure was used for *cis*-dimers as well, but in this case two cadherin extracellular domains were placed on the same surface and their initial orientations were based on the *cis*-interface taken from the C-cadherin crystal structure[15]. The range of domain fluctuations along the z axis, h_C, and the rotational distribution, $\Delta\theta_C$ and $\Delta\psi_C$, were determined and are reported in Supplementary Table 1 and Supplementary Fig. 5.